PCCP

Accepted Manuscript

ROYAL SOCIETY OF CHEMISTRY

www.rsc.org/pccp

RSCPublishing

COMMUNICATION

Flexible Thermoelectric Fabrics Based on Self-assembled Tellurium Nanorods with a Large Power Factor†

DMFCite this: DOI: 10.1039/x0xx00000x

Received,
Accepted

DOI: 10.1039/x0xx00000x

www.rsc.org/

Chaochao Dun,[a] Corey A. Hewitt,[a] Huihui Huang,*[ab] David S. Montgomery,[a] Junwei Xu[a] and David L. Carroll*[a]

Highly-flexible thermoelectric fabrics were fabricated based on a layered structure, composed of a thin active layer of self-assembled tellurium nanorods and a substrate layer of polyvinylidene fluoride. The resulting thermoelectric fabrics show a high room temperature power factor of 45.8 μW/mK^2, which opens a new avenue to fabricate highly-flexible sustainable energy sources.

Nowadays, the large proliferation of portable/wearable electronic devices stimulates research interests in lightweight and highly-flexible renewable and sustainable energy sources like solar cells, piezoelectrics, and thermoelectrics [1-4]. Among them, thermoelectrics provide the unique capability to directly convert heat to electricity, which have the potential to continuously convert body heat into electrical power that could charge the portable/wearable electronic devices. Therefore, the pursuit of high performance flexible thermoelectric power sources is becoming one of the most interesting research fields.

The selection of materials is essential to fabricate high performance and flexible thermoelectrics. Thermoelectric performance of these materials is usually described by the thermoelectric figure of merit, $ZT = \alpha^2\sigma T/\kappa$, where α, σ, T, and κ are the Seebeck coefficient, electrical conductivity, absolute temperature, and thermal conductivity, respectively. By considering the flexible nature of the materials, conductive polymers are thought to be an ideal choice to fabricate highly flexible thermoelectric devices due to the flexible nature and the low thermal conductivity of the polymer [7, 8]; however, most of the conductive polymers like poly(3,4-ethylenedioxythiophene): polystyrene sulfonate (PEDOT:PSS) and poly(3-hexylthiophene-2,5-diyl) (P3HT) are expensive and usually require complex treatments to achieve high electrical conductivity [9, 10]. Another alternative choice for fabricating flexible thermoelectrics is the use of composite materials including conductive nanowires/nanorods and polymers such as carbon nanotube/polymer composites [11-15]. In this case, the carrier transport channel of these materials can be formed by the percolation pathway of the conductive nanostructures, so some cheaper insulating polymers like polyvinylidene fluoride (PVDF) could be selected as the flexible matrix of the composite [16]. However, there is a tradeoff between the electrical conductivity and the flexibility of the composite films. Supposing the nanowires/nanorods are uniformly dispersed in the polymer matrix, in order to get good electrical conductivity, the volume amount of the nanowires/nanorods needs to be high enough to achieve the effective percolation threshold. Conversely, the higher the nanowire/nanorod concentration, the more brittle and less flexible the composite film becomes [12].

In this paper, we use a layered structure to circumvent the dilemma between electrical conductivity and flexibility. The layered structure of the composite is formed by a thin self-assembled inorganic nanorod network layer below the polymer matrix layer. Here, we utilize tellurium (Te) nanorods and PVDF as the inorganic material and the polymer matrix, respectively. Tellurium is a p-type semiconductor with a direct bandgap around 0.35 eV at room temperature. Recently, a theoretical study revealed that Te has the potential to be a good p-type thermoelectric material and its optimum figure of merit ZT could reach 0.31 at room temperature[18]. The resulting thermoelectric fabrics show a high room temperature power factor of 45.8 μW/mK^2, which are an order of magnitude improvement over other Te nanowire based thermoelectircs and comparable to optimized Te nanowire/PEDOT:PSS based thermoelectircs. These results demonstrate its great potential for applications in portable/wearable electronic devices.

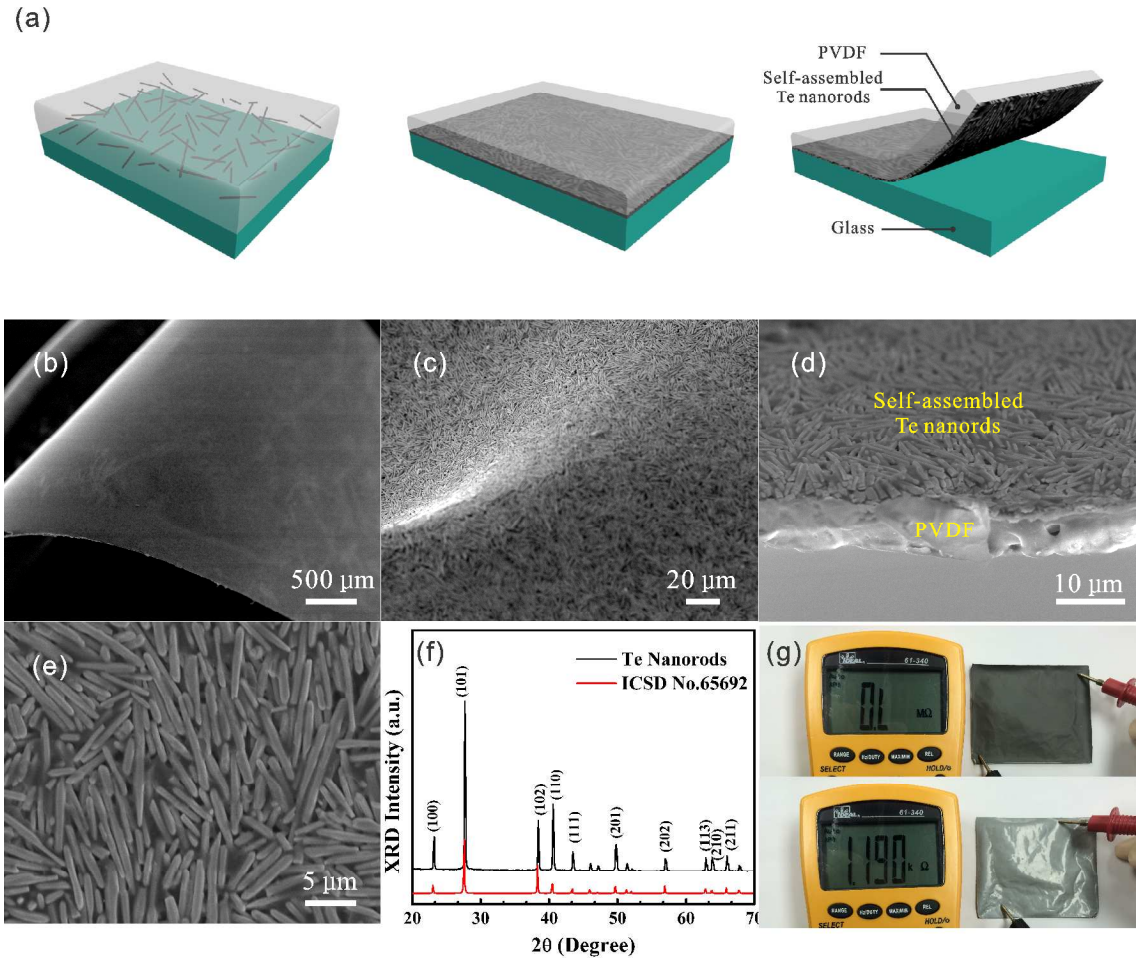

Fig. 1 (a) Schematic of the fabrication process for the self-assembled Te nanorod/PVDF composite based thermoelectric fabrics. (b) SEM image of a curved thermoelectric fabric. (c) High resolution SEM image of a curved thermoelectric fabric. (d) SEM image of the cross-section of a Te nanorod/PVDF thin film. (e) SEM image of the self-assembled Te nanorods on bottom of the thermoelectric fabric. (f) XRD patterns of the as fabricated te nanorods. (g) Two probe surface resistance of the top (top image) and bottom (bottom image) surface of the Te nanorod/PVDF thin film.

The self-assembled Te nanorod/PVDF composites were synthesized using the procedure described in the Experimental section and illustrated in **Fig. 1** (a). The resulting freestanding composites were 66% Te nanorods by weight with a structure consisting of a thin layer of a self-assembled Te nanorod network beneath the PVDF matrix formed during the solvent evaporation process, which should be attributed to the heavy element nature of Te. As shown in **Fig. 1**(b-d), the overall thickness of the composite is around 10 μm, which is composed of approximately 1.5 μm of the self-assembled Te nanorod network and 8.5 μm PVDF. **Fig. 1**(e) shows the bottom-view SEM image of the self-assembled closely packed Te nanorods under the PVDF, with individual Te nanorod lengths of up to 10 μm and diameters of around 600-800 nm. The densely assembled Te nanorods result in the electrical conductivity of the thermoelectric fabrics. It's worth noting that the thin film of the self-assembled Te nanorods are formed of 1-3 layer of closely packed Te nanorods as shown in **Fig. 1**(d). **Fig. 1**(f) shows the x-ray diffraction pattern for the Te nanorods compared to the ICSD standard, demonstrating that the nanorods are in fact Te. **Fig. 1**(g) shows the photographs and surface resistances of the thermoelectric fabrics demonstrating that the Te nanorods form a self-assembled layer on the bottom of the composite as exemplified by the nonconductive top surface. The size of the fabrics shown is 50 mm × 75 mm but is scalable, demonstrating its great potential for compatibility with industry-grade production. Additionally, the thermoelectric fabrics demonstrate high flexibility, which will be specifically discussed below.

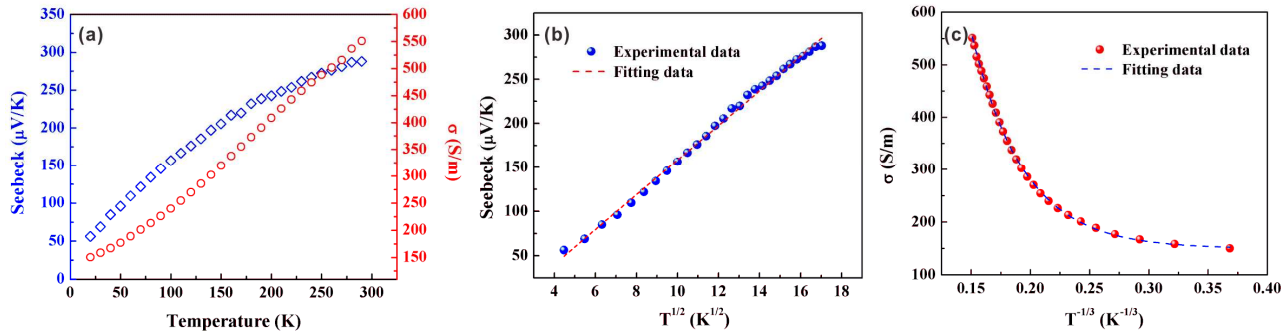

Fig. 2 (a) Temperature-dependent electrical conductivity and Seebeck coefficient of the Te nanorod thermoelectric fabrics plotted in a linear temperature scale. (b) Plot of Seebeck coefficient versus $T^{1/2}$. (c) Plot of electrical conductivity versus $T^{-1/3}$.

The temperature dependent thermoelectric properties of the Te nanorod/PVDF composites were measured from room temperature down to 20 K as shown in **Fig. 2**(a). For the Seebeck coefficient, the room temperature value was +288 μV/K, while that of pure Te nanorods has been measured to be around +408 μV/K. This reduction in values can be explained through the heterogeneous network through the composite consisting of Te nanorods forming conducting pathways through the PVDF matrix. Since the total Seebeck coefficient of the composite is a thermal conductivity weighted average of the coefficients of the Te nanorods and PVDF, and PVDF serves as a barrier to electrical conduction in the rod to rod contacts while reducing the effective total temperature gradient across the nanorods, the measured Seebeck coefficient is reduced. As for the temperature dependent behavior, it also exhibits a heterogeneous composite nature with a decreasing Seebeck coefficient with decreasing temperature and an increasing slope as the values trend towards zero at 0 K. The heterogeneous model is given by

$$\alpha(T) = aT + cT^{1/2}\exp\left[-\left(\frac{T_1}{T}\right)^{1/1+d}\right] \quad (1)$$

where a, and c are constants governing the linear and $T^{1/2}$ contributions, respectively, T_1 is an energy barrier constant for hopping from rod to rod, and d is the dimensionality of the conducting material [19-21]. In this case, a dimensionality of 2 demonstrates the low space-filling percolation network of the Te nanorods [21]. A fit to the data is shown in **Fig. 2**(b). The temperature dependent behavior of the Te nanorods is very similar to that of carbon nanotube/PVDF composites, demonstrating that the mechanism for conduction through heterogeneous conducting pathways is similar despite the conducting material.

For the electrical conductivity of the Te nanorod composites, the room temperature value was 551.6 S/m, which was calculated based on the 4-probe measurements by considering the correction factor as described in the experimental section. This value in conductivity is almost two orders of magnitude greater than that of Te nanowire based thermoelectrics as shown in **Table 1**. This is attributed to the much larger diameters for our Te nanorods. For the temperature dependent behavior, it can be modeled using a variable range hopping model given by

$$\sigma(T) = \sigma_0\exp\left[-\left(\frac{T_1}{T}\right)^{1/1+d}\right] \quad (2)$$

where σ_0 is a constant, and the exponential factor is the same as that in the heterogeneous model describing the temperature dependent Seebeck coefficient behavior. Since the Te nanorods form the conducting network through the PVDF matrix and charge must hop from rod to rod with the aid of thermal energy, as the absolute temperature decreases so too does the electrical conductivity. A fit to the data is shown in **Fig. 2**(c).

The electrical conductivity and Seebeck coefficient combine to yield the power factor given by $\alpha^2\sigma$. The room temperature power factor is about 45.8 μW/mK^2. As shown in **Table 1**, the power factor is an order of improvement than the previously reported Te nanowire based thermoelectrics and comparable to that reported for the

Table 1 Comparison between the room temperature (300 K) performances of as-reported Te nanostructure/polymer based thermoelectrics and the self-assembled Te nanorod/PVDF based thermoelectric fabrics in this work.

	Seebeck Coefficient (μV/K)	Electrical Conductivity (S/m)	Power Factor (μW/mK^2)	References
Te nanowires	408 (±69)	8 (±3)	2.7	[5]
Te nanowires	400	10	1.6	[6]
Te nanowire/PEDOT:PSS	163 (±4)	1930 (±230)	70.9	[5]
Te nanowire/PEDOT:PSS	-	-	100	[6]
Te nanowire/PEDOT:PSS	~150	~200	~4.5	[17]
Self-assembled Te nanorod/PVDF	288	551.6	45.8	This work

optimized Te nanowire/PEDOT:PSS composites. Furthermore, our present composites are composed of a relatively inexpensive nonconducting polymer with low thermal conductivity. If a previously reported value for the thermal conductivity of the Te nanorods of 3 W/mK is used, the estimated *ZT* is about 0.005, however, it is generally recognized that the thermal conductivity can be decreased by improving phonon scattering at the numerous rod to rod boundaries through the use of polymers such as PVDF [22]; thus it is predicted that the real *ZT* of the composite should be much higher than 0.005.

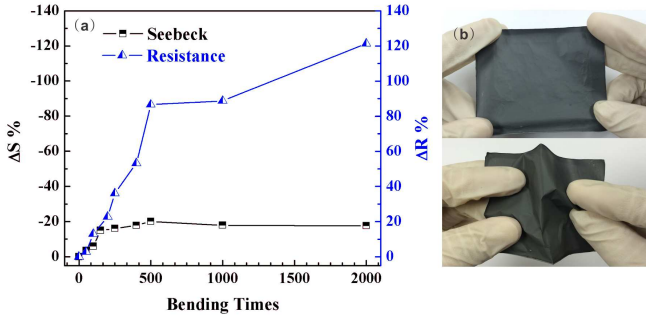

Fig. 3 (a) Reliability of the self-aasembled Te nanorod/PVDF based thermoelectric fabrics. (b) Demonstration of the bending for the reliability test.

An additional benefit of the use of PVDF as the composite matrix is the fact that the resulting film is a free standing, flexible, and durable fabric like composite. The durability of the resulting composite is demonstrated in **Fig. 3**. The film was flexed multiple times as shown in **Fig. 3**(b) with the effects of continual bending on the internal resistance and Seebeck coefficient shown in **Fig. 3**(a). As the number of bending cycles is increased, the internal resistance of the composite increases as well to about double its initial internal resistance by 500 bends before the rate of increase starts to level off. This can be explained by a decrease in the number or quality of the rod to rod junctions as the composite is bent until a maximum degradation in these junctions is reached. Similarly, the Seebeck coefficient decreases slightly by about 20% at 500 bends, where the decrease is also due to the degradation of the rod to rod junctions. Although this test demonstrates that the output of the device is slightly decreased by continual kinetic application, it shows that the performance does level off at only about a 35% total reduction of output in pristine condition.

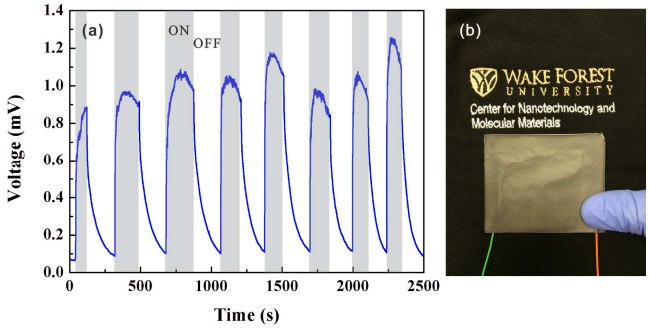

Fig. 4 (a) Fingertip touch response of the flexible thermoelectric fabrics. (b) Demonstration of a themoelectric fabric placed on the clothes that can be activated by fingertip touches.

Finally, as an illustration of the effectiveness of the potential use of these Te nanorod/PVDF composites in thermal energy scavenging applications, **Fig. 4** demonstrates the voltage response of the composite in a touch test. From the thermal energy input from a finger touch, a voltage output of 1 mV is reached, which, from the room temperature Seebeck coefficient, is an estimated supplied temperature difference of about 4 K. The total power output of such a source of thermal energy is dependent on the total available coverable area of thermal radiation. For the human body, that equates to about 2 meters and 100 Watts. With an estimated *ZT* of even 0.005, that equates to a total recoverable power of 4 mW which is sufficient enough to power personal/portable electronics.

In summary, the results presented in this letter demonstrate that self-assembled Te nanorod/PVDF composites exhibit favourable thermoelectric characteristics. The heterogeneous structure of the composites provides several benefits for use in these specific applications. First, the low thermal conductivity nonconducting host polymer matrix serves to bind the conducting Te nanorods together while still maintaining an adequate power factor and figure of merit. Additionally, the physical characteristics of the resulting freestanding Te nanorod/PVDF composites are favourable since they are flexible and durable. At their current performance, if enough thermal energy is available, the composites could be used to provide sufficient thermoelectric power for low powered personal and portable electronics.

Experimental Section

Synthesis of Te Nanorods: Here, Sodium telluride (Na_2TeO_3) was used as the tellurium source. First, 3 mmol Na_2TeO_3 was dissolved in 30 mL ethylene glycol (EG) under vigorous stirring at 130 °C to form a colorless solution. Next, 300 mg $NaBH_4$ was dissolved in 20 ml EG and then added drop by drop to the Na_2TeO_3 solution. Finally, Te nanorods were formed by refluxing the obtained mixture at 290°C for 20 hours. After using isopropyl alcohol to deposite the product, the deposition was collected by centrifugation and purified using actone at least three times. Each cycle lasted 5 minutes at 5000 rpm.

Fabrication of Thermoelectric Fabrics: After drying, nanocomposites consisting of 270 mg Te powder and 135 mg PVDF (ratio 2:1) was disolved in 5 ml Dimethylformamide (DMF, anhydrous 99.8%) and sonicated for 3 hours to ensure uniform dispersion. The solution was then drop-cast on galss and baked on a hotplate at 80 °C overnight in air. The resulting film could then be removed from the glass substrate by soaking in methanol. After removal and drying, the thermoelectric properties of the resulting freestanding Te nanorod/PVDF composite fabrics could be tested.

Characterization: The synthesized Te nanorods were analyzed by XRD using Cu Kα radiation (Bruker D2 Phaser). The morphology and thickness were measured by the Scanning Electron Microscope (JEOL, JSM-6330F). The thermoelectric properties of the Te nanorod/PVDF composites were measured using a custom built apparatus shown in **Fig.** S1 in the supplementary information, similar to that reported by G. T. Kim *et al*. [23]. A typical 4-probe technique was used to measure the electrical conductivity based on the following formula:

$$\sigma = \frac{1}{R} \cdot \frac{l}{S} \cdot \left(\frac{\ln 2}{\pi}\right)$$

where, *R* is the measured 4 probe resistance, *l* is the length, and *S* is the cross section of the samples. The standard correction term was introduced due to the finite dimensions of the probes and boundaries of the sample [24]. The Seebeck coefficient was measured by heating one copper block and simultaneously measuring ΔT and the thermoelectric voltage generated. This system was calibrated using a standard constantan sample, including the subtraction of the contribution from the gold plated voltage probes.

Acknowledgements

This study was conducted under support from the Air Force Office of Scientific Research Grant Number FA 9550-13-1-0085.

Notes and references

[a]*Center for Nanotechnology and Molecular Materials, Department of Physics, Wake Forest University, Winston-Salem, NC 27109, U. S. E-mail: huangh@wfu.edu; carroldl@wfu.edu*

[b]*SZU-NUS Collaborative Innovation Center for Optoelectronic Science & Technology, Key Laboratory of Optoelectronic Devices and Systems of Ministry of Education and Guangdong Province, College of Optoelectronic Engineering, Shenzhen University, Shenzhen 518060, China.*

† Electronic Supplementary Information (ESI) available: Experimental setup for the thermoelectric measurement (**Fig.** S1); Temperature-dependent power factor of the thermoelectric fabrics (**Fig.** S2). See DOI: 10.1039/c000000x/

1. Z. Fan, H. Razavi, J.-w. Do, A. Moriwaki, O. Ergen, Y.-L. Chueh, P. W. Leu, J. C. Ho, T. Takahashi, L. A. Reichertz, S. Neale, K. Yu, M. Wu, J. W. Ager and A. Javey, *Nat Mater*, 2009, **8**, 648-653.
2. J. Yoon, A. J. Baca, S.-I. Park, P. Elvikis, J. B. Geddes, L. Li, R. H. Kim, J. Xiao, S. Wang, T.-H. Kim, M. J. Motala, B. Y. Ahn, E. B. Duoss, J. A. Lewis, R. G. Nuzzo, P. M. Ferreira, Y. Huang, A. Rockett and J. A. Rogers, *Nat Mater*, 2008, **7**, 907-915.
3. R. Yang, Y. Qin, L. Dai and Z. L. Wang, *Nat Nano*, 2009, **4**, 34-39.
4. C. A. Hewitt, A. B. Kaiser, S. Roth, M. Craps, R. Czerw and D. L. Carroll, *Nano Letters*, 2012, **12**, 1307-1310.
5. K. C. See, J. P. Feser, C. E. Chen, A. Majumdar, J. J. Urban and R. A. Segalman, *Nano Letters*, 2010, **10**, 4664-4667.
6. S. K. Yee, N. E. Coates, A. Majumdar, J. J. Urban and R. A. Segalman, *Physical Chemistry Chemical Physics*, 2013, **15**, 4024-4032.
7. O. Bubnova, Z. U. Khan, A. Malti, S. Braun, M. Fahlman, M. Berggren and X. Crispin, *Nature Materials*, 2011, **10**, 429-433.
8. D. Kim, Y. Kim, K. Choi, J. C. Grunlan and C. Yu, *ACS Nano*, 2009, **4**, 513-523.
9. G. H. Kim, L. Shao, K. Zhang and K. P. Pipe, *Nat Mater*, 2013, **12**, 719-723.
10. M. Chabinyc, *Nat Mater*, 2014, **13**, 119-121.
11. C. A. Hewitt and D. L. Carroll, *Synthetic Metals*, 2012, **162**, 2379-2382.
12. C. A. Hewitt, A. B. Kaiser, M. Craps, R. Czerw, S. Roth and D. L. Carroll, *Synthetic Metals*, 2013, **165**, 56-59.
13. J. Liu, A. Rasheed, M. L. Minus and S. Kumar, *Journal of Applied Polymer Science*, 2009, **112**, 142-156.
14. C. Yu, K. Choi, L. Yin and J. C. Grunlan, *ACS Nano*, 2011, **5**, 7885-7892.
15. C. Yu, Y. S. Kim, D. Kim and J. C. Grunlan, *Nano Letters*, 2008, **8**, 4428-4432.
16. C. A. Hewitt, A. B. Kaiser, S. Roth, M. Craps, R. Czerw and D. L. Carroll, *Applied Physics Letters*, 2011, **98**, 183110.
17. S. Ma, K. Anderson, L. Guo, A. Yousuf, E. C. Ellingsworth, C. Vajner, H. T. Wang and G. Szulczewski, *Applied Physics Letters*, 2014, **105**, 073905.
18. H. Peng, N. Kioussis and G. J. Snyder, *Physical Review B*, 2014, **89**.
19. Y.-M. Choi, D.-S. Lee, R. Czerw, P.-W. Chiu, N. Grobert, M. Terrones, M. Reyes-Reyes, H. Terrones, J.-C. Charlier, P. M. Ajayan, S. Roth, D. L. Carroll and Y.-W. Park, *Nano Letters*, 2003, **3**, 839-842.
20. A. B. Kaiser, G. Düsberg and S. Roth, *Physical Review B*, 1998, **57**, 1418-1421.
21. D. L. Carroll, R. Czerw and S. Webster, *Synthetic Metals*, 2005, **155**, 694-697.
22. C. J. Vineis, A. Shakouri, A. Majumdar and M. G. Kanatzidis, *Advanced Materials*, 2010, **22**, 3970-3980.
23. G. T. Kim, J. G. Park, J. Y. Lee, H. Y. Yu, E. S. Choi, D. S. Suh, Y. S. Ha and Y. W. Park, *Review of Scientific Instruments*, 1998, **69**, 3705-3706.
24. E. J. Zimney, G. H. B. Dommett, R. S. Ruoff and D. A. Dikin, *Meas. Sci. Technol.*, 2007, **18**, 2067-2073.